Doublet tracer tests to determine the contaminant flushing properties of a municipal solid waste landfill

Woodman, N. D.*, Rees-White, T. C. Beaven, R. P. Stringfellow, A. M. & Barker J.A.

Faculty of Engineering and the Environment, University of Southampton, Southampton, SO17 1B, UK.
*Corresponding author

Keywords

Doublet, tracer, municipal solid waste, flushing, dual-porosity

Highlights

- Closed-loop doublet tracer tests are effective at characterising transport in waste
- Transport in waste is predictable using a double-continuum dual-porosity model.
- Diffusion is likely to be rate-limiting for solute-flushing from landfill sites.

Abstract

This paper describes a programme of research investigating horizontal fluid flow and solute transport through saturated municipal solid waste (MSW) landfill. The purpose is to inform engineering strategies for future contaminant flushing. Solute transport between injection/abstraction well pairs (doublets) is investigated using three tracers over five separate tests at well separations between 5 m and 20 m. Two inorganic tracers (lithium and bromide) were used, plus the fluorescent dye tracer, rhodamine-WT. There was no evidence for persistent preferential horizons or pathways at the inter-well scale. The time for tracer movement to the abstraction wells varied with well spacing as predicted for a homogeneous isotropic continuum. The time for tracer movement to remote observation wells was also as expected. Kinematic (mobile) porosity was estimated as ~0.02 (~4% of total porosity). Good fits to the tracer breakthrough data were achieved using a dual-porosity model, with immobile regions characterised by block diffusion timescales in the range of about one to ten years. This implies that diffusional exchanges are likely to be very significant for engineering of whole-site contaminant flushing and possibly rate-limiting.

1. Introduction

Landfilling remains the main disposal method for municipal solid waste (MSW) globally. Of the estimated 1.3 billion tonnes of MSW produced in 2012, the majority ended up in landfills or open dumps (Bhada-Tata *et al.*, 2012). Even where landfilled volumes are reducing (such as within the EU) it is very likely that there will be a continued need to dispose of 'residuals'.

The leachate generated by landfills represents a potential pollution risk to groundwater and surface water bodies (e.g. Christensen *et al.*, 2011; Turner *et al.*, in press). This liablity will often last for many centuries after a site has closed (Hall *et al.*, 2004) and requires ongoing active aftercare to manage the risk. This potential burden to future generations contradicts one of the core principles of sustainable development, i.e. that the problems of today should not be passed on to future generations (United Nations, 1987). Since it is broadly recognised that landfill engineering systems

will deteriorate in the long term (Drury *et al.*, 2003; Rowe, 2005) there is a case for engineering *in situ* clean-up of existing sites to reduce the legacy handed to future generations (e.g. Scharff *et al.*, 2011; Beaven *et al.*, 2014; Kattenberg *et al.*, 2013).

Concern over the potential for contaminant leakage from landfills has resulted in leachate heads often being kept at a low level within the waste and thus the majority of the waste in managed landfills is unsaturated. Nonetheless, where the landfill basal drainage system is non-existent or malfunctioning (for example, clogged), vertical wells are frequently used for leachate extraction in landfills to reduce water levels and control hydraulic heads. In many older landfills in the UK, significant depths of saturated waste exist (and are permitted) in sites benefiting from natural containment created by surrounding geology with low permeability. Although there are presently regulatory barriers to raised leachate tables, increasing water levels would potentially encourage greater microbial activity and allow a higher flushing efficiency (Beaven *et a*l., 2004). In such cases vertical wells could be used to provide an accelerated flushing of the waste. This could be achieved by inducing flow within the landfill between vertical wells. Clean water would be injected into one or more wells and leachate pumped out from others. Such systems are used for contaminant clean up in soils (e.g. Lee *et al*., 2014).

The basic hydraulic unit for the flow system produced from such systems is a well-pair doublet, whereby fluid is injected at one well and abstracted at a second one at the same rate. Proper understanding of a flow and solute movement in a doublet unit can potentially be applied to the design of a system of multiple-wells for flushing the site at full-scale.

Given previous difficulties interpreting pumping tests in waste (Burrows *et al.*, 1997; Burrows, 1998; Cossu *et al*. 1997; Rees-White, 2007; Giardi, 1997) it is conceivable that the complexities of an actively degrading waste body may make pumping between wells difficult to characterise. Furthermore, it is possible that heterogeneity causes a highly non-uniform flow which results in a less effective sweep of the waste mass than would have occurred in a uniform flow regime. Heterogeneities within the waste may concentrate flow within discrete horizons, isolating the remaining saturated thickness from the flow of clean water. Reductions in hydraulic conductivity with depth due to increasing overburden may cause systematic reductions in flow rates with depth (Powrie & Beaven, 1999), reducing the flow and therefore clean-up rate for the deeper layers. For wells too close together, fast pathways could potentially be created between wells causing short-circuiting. For more widely spaced well-pairs, larger-scale heterogeneities and even the boundaries of the landfill cell may affect the flow. Consequently, there is a need for the quantification of how uniformly between-well flow passes through saturated waste both in vertical and lateral extent.

This paper uses artificial tracers to reveal the dynamics of fluid movement within doublets at different scales. This allows a number of questions to be addressed: How well does an idealised homogenous porous medium assumption predict water movement in a doublet within MSW? Can short-circuiting be observed between wells? What is a practical scale to flush landfills using wells?

The overarching aim of this paper is therefore to provide a quantification of the nature of flow and transport of leachate in a doublet well-pair at a range of scales in a (MSW) landfill site. Specifically we aim to test the hypothesis that a doublet in MSW can be reliably simulated using a continuum mass-transport model.

2. Methodology

2.1. Field site and method

The tests were carried out at a 66 ha restored landfill located in an old clay quarry in Southern England which had been excavated to a depth of approximately 19 metres below surrounding ground levels (at ~14 m OD). The earliest waste was deposited in the 1980s and landfilling continued until the site was completed in 1996, having accumulated ~20 M tonnes of predominantly MSW and commercial/ industrial wastes. Restoration took the form of a 1 m rolled-clay cap and protective soil layer with a minimum depth of 1.8 m. The final landform was a dome-shaped land-raise with a current maximum elevation of ~15 mOD and an average waste depth of ~27 m.

The contours of the base of the site are close to being horizontal and there is no basal liner or drainage system. Leachate extraction is in the order of 1,500 m^3/year, collected from vertical wells installed with submersible pumps. The closest pumped well to the test wells is ~100 m away, from which up to 100 m^3 is extracted annually. The saturated depth was 17.2 m on average during the three-year experimental period. Current gas extraction is between 800 – 1,000 m^3/h.

The area used for the tests reported herein surrounded an existing 180 mm ID leachate abstraction well ('AW'). Four new 150 mm ID wells (A to D) and two 58 mm ID observation wells (O1 and O2) were installed. Wells A to D were fully screened within the saturated zone whereas the observation wells were screened over a much narrower depth interval (O1 from -11.1 to 10.1 mAOD and O2 -2.4 to -1.4 mAOD). Figure 1 shows the relative positions of the wells and Table 1 details each well. The abstraction and injection wells A to C were close to fully penetrating the entire saturated thickness. All doublet tracer tests followed the same general method. Leachate was pumped from the abstraction Well (AW) at a constant flow rate and injected back into one of Wells A, B or C (D was not used) via 272 m of 40.8 mm internal diameter pipe which passed through a control room. The control room was located on the edge of the site approximately 130 metres from the testing field. The flow rate in all tests was controlled to a constant 47.7 m^3/d (~2 m^3/h) using a PID controller that used the output from an electromagnetic flowmeter (Endress + Hauser, Promag 50) to operate an actuated valve (Samson V2001-3321-E3) in the flow line. The advection time in the pipe between wells was therefore relatively rapid (0.07 h). Prior to each individual tracer test there was a period of pumping to allow hydraulic equilibration and where background concentrations of the tracers were monitored in-line at the abstraction well and from point samples taken at observation wells. When hydraulic equilibrium had been reached, tracer(s) were injected into the recirculation pipework in the control room and pumped into the landfill at the relevant injection well. A summary of tests undertaken is provided in Table 2.

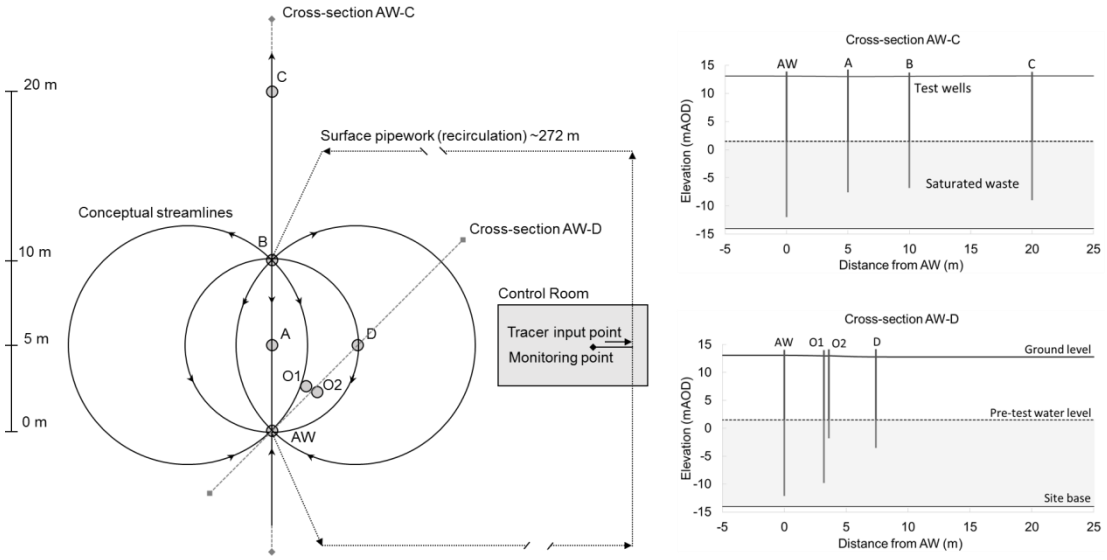

Figure 1: Borehole and monitoring network showing conceptual streamlines during pumping. Cross-sections through wells AW-C and AW-D show the relative position and depth of the test wells and the pre-test saturated level of the waste.

Table 1: Borehole details.

Well	Distance from well AW (m)	Well Diameter (mm)	Depth of water in well prior to test programme (m)	Saturated depth of waste prior to test programme (m)
AW	0.0	180	13.6	15.4
A	5.1	150	8.9	15.3
B	10.0	150	8.1	15.3
C	19.9	150	10.3	15.3
D	7.4	150	4.7	15.7
O1	3.5	58	11.3	15.6
O2	3.8	58	3.3	15.6

Table 2: summary of tracer tests.

Test	Tracer	Injection well	Distance to AW (m)	Prior hydraulic equilibration time (days)	Duration (days)	Flow rate Q (m^3/d)	Observation well data
1	Bromide	B	10	21	70.9	47.7	None
2	RWT	C	19.9	20	58.0	47.9	None
3	Lithium	C	19.9	10	62.9	47.9	Point samples taken at -1.6 mAOD
4	Lithium	A	5.1	11	52.0	47.9	Point samples taken at -1.6 mAOD
	Bromide	A	5.1	11	52.0	47.9	Point samples taken at -1.6 mAOD
5	RWT	A	5.1	11	83.0	47.9	500 mm interval vertical profile

2.2. Selection of tracers

Tracer testing in landfills is challenging due to the high ('background') concentration of most elements within the leachate, the reactive nature of leachates and the multi-component nature of the waste medium (Blakey *et al.*, 1998; Woodman, 2007). Given this heightened chance of reaction, there is an

advantage in using multiple tracers in the investigation to provide a means to establish whether tracers are behaving conservatively, or otherwise.

Therefore, three different tracers were selected for injection into the doublet systems: Rhodamine WT (RWT), bromide, and lithium. The details of the tracers and the quantities injected are given in Table 3.

Table 3: tracer injection details. [*placed at end of document; landscape format*]

Rhodamine WT (RWT) was selected as a tracer that can be rapidly and cheaply monitored, inline in the pumping circuit and for high-resolution depth profiling using a down-well fluorometer (Cyclops-7, Turner Designs). The suitability of different fluorescent dyes for use as tracers in landfills was examined in Marius *et al.* (2010). Despite the deep colour and high fluorescence of humic and fulvic acids present in leachate dissolved organic matter, RWT, Fluoroscein and Eosin may be uniquely distinguished against leachate fluorophores. Organic dyes cannot be guaranteed to behave as 'ideal tracers', being subject to biochemical degradation in the landfill (Smart, 1985, Blakey *et al*., 1998) and sorption (Marius *et al*., 2010). RWT was shown to be the most suitable of these three tracers in anaerobic landfill conditions, exhibiting less degradation than Eosin and more linear sorption in comparison to Fluoroscein (Marius *et al*., 2010).

Bromide (Br) tracer is observed to behave conservatively in some media (Flury and Flühler, 1995), although this cannot be guaranteed given the reactive nature of MSW and leachate. Bromide was shown to be conservative as tracer through saturated MSW in a large-scale experimental column cell being flushed with clean water in comparison to other flushed species (Woodman *et al*., 2015).

Lithium (Li) has been used several times as a tracer for transport within MSW (Blakey *et al*., 1998; Öman and Rosqvist, 1999; Rosqvist & Bendz, 1999; Beaven *et al.*, 2001; Beaven *et al*., 2003). Its common use in MSW is explained by its relatively low cost and commonly low background concentration (Harris, 1979; Blakey *et al*., 1998). Batch tests have not shown significant sorption of lithium in leachate onto MSW (Stegemann *et al*., 2006; Öman and Rosqvist, 1999). However, recent non-conservative behaviour of lithium has been reported in MSW under different laboratory conditions (Woodman *et al*., 2013, Woodman *et al*., 2014; Woodman *et al*., 2015). It was consistently found that there was a loss of lithium in tracer tests in gassing wastes, however the mechanism responsible for this remains unexplained.

2.3. Sampling and analysis

The concentration of tracers entering the landfill was monitored from samples taken at the injection well. Samples from the recirculating leachate were collected in the control room (Figure 1) either manually, from a sample tap in the recirculation pipework, or automatically using an autosampler (Endress & Hauser, Liquiport 2000 RPT20). Where the autosampler was used, 1 litre of sample was collected, from which 250 or 500 ml was decanted into a pre-rinsed plastic (PET) bottle for storage and analysis. All samples were refrigerated after sampling.

Samples from wells and piezometers were collected using a manual inertial pump (Waterra UK), with the tube inlet located ~12 m from the base of the landfill (at ~-1.6 mAOD) in each well to ensure that sampling was always from the same waste horizon. Approximately 2 litres of liquid was purged prior to any sampling. Samples were collected in 250 or 500 ml plastic (PET) bottles, which were rinsed out with a pre-sample of the liquid being collected prior to being filled to the brim and capped.

Downhole RWT profiling was carried out using a Cyclops-7 rhodamine fluorometer (Turner Designs) attached to a CR10X datalogger (Campbell Scientific) with real-time output. Measurements were made at 0.5 m intervals throughout the full saturated depth of the well.

For analysis of inorganic tracers, a sub-sample of between 10-20 ml was filtered (Whatman 0.45 µm glass-fibre filter) and fixed with 0.6 ml 33 % nitric acid. Sub-samples were diluted 1:100 with 2 % Nitric acid (trace analysis grade) and analysed for metals and a range of ions using an ICP-MS (Thermo-Scientific X-series). In Test 4, samples were analysed without prior filtering or preservation with acid. Rhodamine tracers were analysed in the laboratory using a fluorescence spectrophotometer (Cary Eclipse). Samples were diluted 1:100 and analysed at 20 °C.

2.4. Prior flow and transport characterisation tests

Prior to the installation of the monitoring wells, flow and transport characterisation tests were performed in the pumping well used in the tracer experiments and in two adjacent leachate extraction wells (within 100 m of the test well). Wells were pumped for between 6 and 7 hours at a constant discharge rate and drawdown and recovery data was analysed using the Theis (1935) solution. This established a bulk estimate for hydraulic conductivity of between K= 1.7 x 10^{-4} m/s and 2.4 x 10^{-5} m/s (1.5 x 10^{-5} m/s in the test abstraction well, 'AW').

A number of borehole dilution tests were performed prior to the doublet tests (Rollinson *et al*., 2010). These are available in the supplementary information to this paper.

Firstly, borehole dilution tests were performed in wells A to C prior to the doublet tests to characterise ambient hydraulic conditions of flow. The tracer rhodamine WT (RWT) was injected along the length of each well and profiles of fluorescence with depth were measured over time (Rollinson *et al*., 2010). Based on these profiles, the Darcy velocity, q, of the 'regional flow' at each depth in this un-pumped state was estimated by $q = \pi r_w s_d/4$ where r_w is the well radius (e.g. Ward *et al*., 1998) and s_d is the slope of a plot of ln(c) against time. Horizontal flow and perfect mixing in the waste was assumed. The range in velocity in wells A, B and C was small (0.004-0.006, 0.005-0.006, 0.005-0.008 m/d respectively) and with no systematic depth trend.

Three borehole dilution tests were performed in well A using RWT during doublet flow between AW and well B (i.e. with a 'forced gradient') prior to the main tests at three different flow rates. An incoherent pattern was seen in the 1 m^3/h test. In the 2 m^3/h test slightly relatively elevated flow velocities at the shallower depths were implied, but this was less distinct at 3 m^3/h. There were no strongly indicated preferential horizons.

'Point dilution' tests were used to check on vertical flow rates in wells A and D during pumping between AW and well B at 2m^3/h. Fluorescein dye tracer was injected at specific single depths in each well and the vertical migration of tracer to other parts of the well monitored. A significant vertical flow would be expected to move tracer up or downwards in the well away from the point of injection. However, using this method, no vertical flow was detected (i.e. the lateral movement out of the well was much more significant than any vertical flow). This is unsurprising, since the injection and abstraction wells were applying a constant head with depth.

Because this is a relatively shallow landfill, yet with a high leachate level, the estimated change in effective stress over the saturated zone is modest. Using the Powrie & Beaven (1999) relationship to predict hydraulic conductivity based on effective stress; $K = 2.1\sigma'^{-2.71}$, K is predicted to drop from

4×10^{-6} to 3×10^{-6} m/s from 10 m to 20 m depth[1]. A modest reduction in flow rate with depth would therefore be anticipated and would be consistent with the forced-gradient dilution tests in the presence of more random heterogeneity. Overall, the dilution data show no evidence of pronounced short circuiting, nor sustained occurrence of preferential flow along any individual horizon. There is a relatively small reduction in flow rate with depth.

Finally, in advance of the doublet tracers tests, injection and withdrawal ('echo') tracer tests were used to characterise the transport properties close to the pumping well (Rees-White *et al*, 2014). Approximately 6 m^3 were injected in to AW in each of two tests and then withdrawn. Analyses of these tests were indicative of dual porosity flow (Rees-White *et al*., 2016, in prep.).

In summary, prior hydraulic and tracer characterisation tests of the area where the doublet tests were to be performed revealed a relatively slow-moving ambient flow. No systematic variability in flow with depth was identified and no persistent preferential horizons were found. Whilst flow is relatively well distributed though the saturated depth, more localised dual porosity effects are indicated by echo tests.

2.5. Transport model

The conceptual model developed here (Figure 2) is based on the geometry of the system shown in Figure 1. Solute transport through the major hydraulic components is represented by transfer functions (e.g. Jury & Roth, 1990) and given here in the Laplace domain.

The transport behaviour of primary interest is that through the waste. The bulk transport behaviour in the waste for flow between the wells is represented by the transfer function $\mathrm{W}(s)$, where *s* is the Laplace variable (hereafter, we write as W). This transfer function is established by first evaluating the pattern of liquid flow between the wells. This flow field can be envisaged as comprising an infinite set of streamlines running between the injection and abstraction wells.

The flow between two wells pumping in and out at equal rates has been extensively studied for pure fluid advection (Muskat, 1937), in the presence of mechanical dispersion (Hoopes & Harleman 1967), where there is dual-porosity exchange (Becker & Shapiro, 2000; Barker, 2010) and where regional groundwater advection is superposed with the flow induced by the doublet (Luo & Kitanidis 2004). Here, the results given in Barker (2010) for dual-porosity transport are extended to a closed-loop flow system.

Firstly, to estimate the advective travel time distribution based on the flow-field, it is assumed:

- The wells are vertical and are screened through the full saturated depth.
- The wells pump at equal and opposite constant rates giving steady-state hydraulic conditions.
- The formation is confined (or the water table horizontal), homogeneous and laterally-isotropic, and of infinite extent.
- The wells are of infinitesimal diameter.
- Regional flow rates are negligible.

These assumptions allow subsequent calculation of the advective travel times associated with each streamtube within the waste as a function of the angle, ψ, that the streamtube meets the line between the two wells, at the abstraction well (i.e. $t_a(\psi)$). More details of this are given in Barker (2010). The fastest pathway (taking minimum time, t_b) is along the direct line between the wells

[1] Assuming 20 kPa overburden from cover layer and 10m unsaturated zone, with γ=11 kN/m^3

(where $\psi = 0$). This characteristic travel time is a function of the well spacing (D), saturated thickness (b), kinematic porosity (θ_k) and pumping rate (Q):

$$t_b = \frac{\pi D^2 b \theta_k}{3Q} \quad [1]$$

The slowest travel times are in the streamtubes that align with the two wells and end in stagnation points, taking in theory an infinitely long period to reach the abstraction well. Advective transport through a doublet arrangement from injection well to abstraction well therefore disperses solute, producing long (theoretically infinite) tails of solute arrival times at the abstraction well.

The solute tracers are simulated as being conservative (i.e. without reaction, for example decay or sorption). However, there are further dispersive mechanisms. These are conceptualised as acting along each streamtube and is assumed to be negligible between streamtubes. In particular, dispersion arises from mechanical dispersion and diffusive transfer.

Mechanical dispersion is due to heterogeneity of flow velocities. It is assumed that for transport within saturated MSW these effects can be lumped in to a (Fickian) macroscopic dispersivity, whereby the solute spreading is proportional to distance along the streamtube pathway (i.e. this is the advection-dispersion (AD) streamtube model.)

There is growing evidence that the predominant mechanism responsible for dispersion of solutes in waste is diffusive exchange between portions of waste which are relatively permeable to waste and regions in which water is less mobile (Beaven *et al.*, 2003; Rosqvist & Bendz, 1999; Fellner & Brunner, 2010; Woodman, 2007; Woodman *et al*. 2013, 2015). Given that MSW contains a mixture of materials, including low-permeability objects (for example, plastics) it would be unsurprising that instead of the sort of uniform flow anticipated for a granular medium that less mobile (or immobile) areas of waste will occur and flow will occur along preferential pathways (the mobile zone). An idealisation that arises from these observations, is that of a 'dual-porosity' medium, whereby there are assumed to be two overlapping continua (mobile and immobile zones of liquid) between which solute is exchanged by diffusion. Both zones are assumed to be homogeneous and isotropic, with advection only occurring in the mobile zone. This process may be simulated independently ('DP') or in addition to mechanical advection-dispersion in the mobile zone ('AD-DP').

To develop a DP model, the geometry of the immobile zone must be assumed. In practice, the shape of blocks is unknown, the internal structure of MSW being notoriously difficult to determine. Previous experience has demonstrated that a single assumed geometry is sufficient to model tracer data in MSW adequately, no doubt the real geometry being simulated by a lumped set of apparent parameters (Woodman, 2007). We may make an informed guess as to a reasonable shape. Compression, primarily from the overburden of layers above, tends to produce sub-horizontal layering of plastics which may promote preferential flow (Bendz & Singh, 1998), and thereby leaving slab-like zones of less mobile waste between them (Woodman *et al*.,2014).

Solute transport within the pumping wells is modelled by assuming instantaneous mixing of the free-water within each well with the water incoming into the well. ~~Where water ingress into (or out of) the well is not uniform but via discrete horizons, potentially not all the well volume would be involved in mixing and can be simulated by lowering the assumed mixing volumes (and hence mixing times).~~

Between the wells water (leachate) is recirculated in 272 m of 40.8 mm ID surface pipework, via a monitoring point at the half-way point. Since negligible longitudinal dispersion is anticipated (the Reynolds number in the pipe is ~17,000, applying Taylor's (1954) equation for a pipe gives α~0.012 m), the transfer function between the abstraction well and the injection well is for pure

advection. The travel time for transport to the monitoring point (t_M) is half that to the injection well (t_R).

The recirculation has a significant effect on the tracer breakthrough curve (BTC) in comparison to tracer test where there was no recirculation. Tracer which has already travelled through the system is fed back into the waste at the injection point. Concentrations at the monitoring point would therefore be expected to both rise more rapidly than in the event that there was no recirculation and also fall more slowly after the peak.

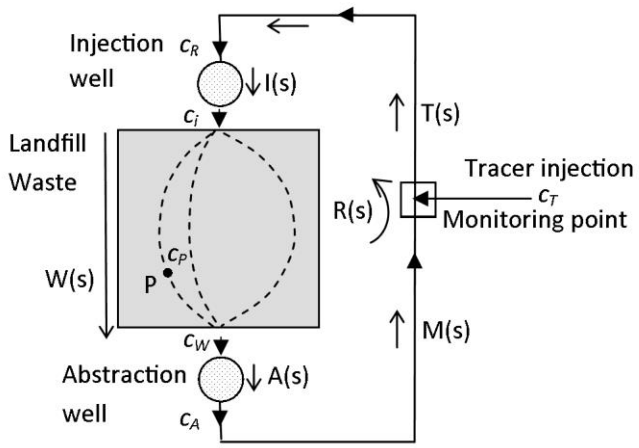

Figure 2: Conceptual model of flow and transport. Transfer functions (TF) for the model (s is the Laplace variable, R is the return TF from the abstraction well to the injection well, M is the TF from abstraction well to monitoring point, T is the TF from the monitoring point to the injection well, I is the (well-mixed) TF for the injection well, W is the TF for the flow through the waste, A is the (well-mixed) TF for the abstraction well.

Given the arrangement of transfer functions in the closed-loop system depicted in Figure 2, the modelled tracer concentration above background at the monitoring point is given by:

$$\bar{c}_M = \frac{\mathrm{MTW}\bar{c}_T}{(1+st_I)(1+st_A) - \mathrm{RW}} \quad [2]$$

Where t_I and t_A are the (perfect) mixing timescales for the injection and abstraction wells respectively (which have initial concentration equal to the background concentration, C_b), R is the transfer function for the return pipework back to the injection well (for systems where there is no recirculation, R=0), W is the transfer function for the waste and s is the Laplace variable. The (background-corrected) input tracer concentration is given by $\mathrm{c}_T = \mathrm{C}_T - \mathrm{C}_b$. The initial concentration in the pipework is also assumed to be equal to background.

Since a negligible dispersivity is anticipated, the transfer function for pure advection in the pipework from AW to the injection well is used:

$$\mathrm{R} = \exp(-st_R) \quad [3]$$

Including dispersion in [3] would be straightforward for any application that required it.

The distribution of advection times in a doublet is given by (Barker, 2010):

$$t_a(\psi) = 3t_b(1 - \psi\cot\psi + \cot^2\psi + \psi\cot^3\psi) \quad [4]$$

where t_b is the characteristic advection time between the wells (given by Equation [1]).

The transfer function for transport though the waste from the injection well to the abstraction well is given as an integral over the streamlines (defined by the angle between the streamline at the abstraction well and the line between the wells, ψ), for $t > t_b$:

$$\mathrm{W} = \frac{1}{\pi}\int_0^{\psi_t} \bar{f}_\delta(\psi)d\psi \quad [5]$$

where ψ_t is given by the solution of: $t_a(\psi_t) = t$. We examine different possible forms of dispersive response ($\bar{f}_\delta$).

For only the dual-porosity (DP) process acting:

$$\bar{f}_\delta(\psi) = \exp\left[-st_a(\psi)\left(1 + \sigma\mathrm{B}\left(\sqrt{st_{cb}}\right)\right)\right] \quad [6]$$

where t_{cb} is the characteristic block diffusion time. The Block Geometry Function, B (Barker, 1985) for Fickian diffusion in and out of a block is purely a function of the shape of the immobile zone. Here, a 'slab' geometry is adopted (i.e. blocks of immobile waste conceptualised as parallel plate-like layers), such that:

$$\mathrm{B(x)} = \tanh(x)/x \quad [7]$$

σ is defined as the ratio of immobile (θ_{im}) to mobile (θ_m) water, i.e. $\sigma = \theta_{im}/\theta_m$. The total water content is comprised of the sum of these mobile and immobile volumetric fractions, i.e. $\theta = \theta_{im} + \theta_m$.

Alternatively, assuming only mechanical dispersion is occurring (i.e. the advection-dispersion model - 'AD'), and without any 'back-dispersion' from the abstraction well:

$$\bar{f}_\delta(\psi) = \exp\left[\left(1 - \sqrt{1 + 4\alpha_L st_a(\psi)}\right)/2\alpha_L\right] \quad [8]$$

Where α_L is the streamwise dispersivity divided by the distance *z* travelled along the streamline and is assumed to be constant.

Assuming the same boundary conditions but additionally assuming mechanical dispersion and dual-porosity effects act simultaneously ('AD-DP'), is given by:

$$\bar{f}_\delta(\psi) = \exp\left[\left(1 - \sqrt{1 + 4\alpha_L st_a(\psi)\left(1 + \sigma\mathrm{B}\left(\sqrt{st_{cb}}\right)\right)}\right)/2\alpha_L\right] \quad [9]$$

The concentration of tracer at any point, P in the waste above background, is:

$$\bar{c}_P = \bar{c}_I\bar{f}_\delta \quad [10]$$

where travel time $\tau(\psi)$ in Equation [5] is replaced by the travel time from the injection well to P and the concentration at the injection well is given by:

$$\bar{c}_I = \frac{\bar{c}_T(1 + st_A)}{(1 + st_I)(1 + st_A) - \mathrm{RW}} \quad [11]$$

The tracer input is modelled as a constant concentration 'pulse' (or 'top-hat'), which lasts for a finite period of time, t_T.

Concentrations at different times are found by numerically inverting these Laplace-transformed concentrations into the time domain.

To optimise these models against the field tracer tests, the sum of the square errors between the model and concentration data is minimised by gradient descent. The Hessian matrix is then computed at the optimum to allow estimation of the standard error of each parameter of the fit (Press *et al*., 1992).

3. Tracer test results and analysis

The tracer data are now examined hierarchically, starting with observations of the breakthrough curves at the abstraction well. The conservative nature of the tracers is assessed by comparison between the tracers. The times of first arrival at the abstraction and observation wells in the different tests are both used to assess the extent to which the flow patterns conform to that of idealised doublets. In addition, the distribution of tracer is examined through the saturated depth at the observation wells, therefore giving an assessment of the uniformity of tracer movement. The knowledge built up from these observations is used to check on the validity of the modelling assumptions. Thus validated, the late-time gradients of the BTCs are analysed and finally entire BTCs are simulated with models.

3.1. Shapes of breakthrough curves (BTCs)

The breakthrough curves (Figure 3a) all exhibit a similar shape: a rapid breakthrough (first detection occurring within hours in tests lasting >50 days), followed by a steep rise in concentration to a peak, which then descends into a tail. The consistency of the BTCs suggests an absence of large-scale heterogeneities and that between-well transport through the waste medium might be reasonably represented by an REV at the three scales examined here (5, 10 and 20 m).

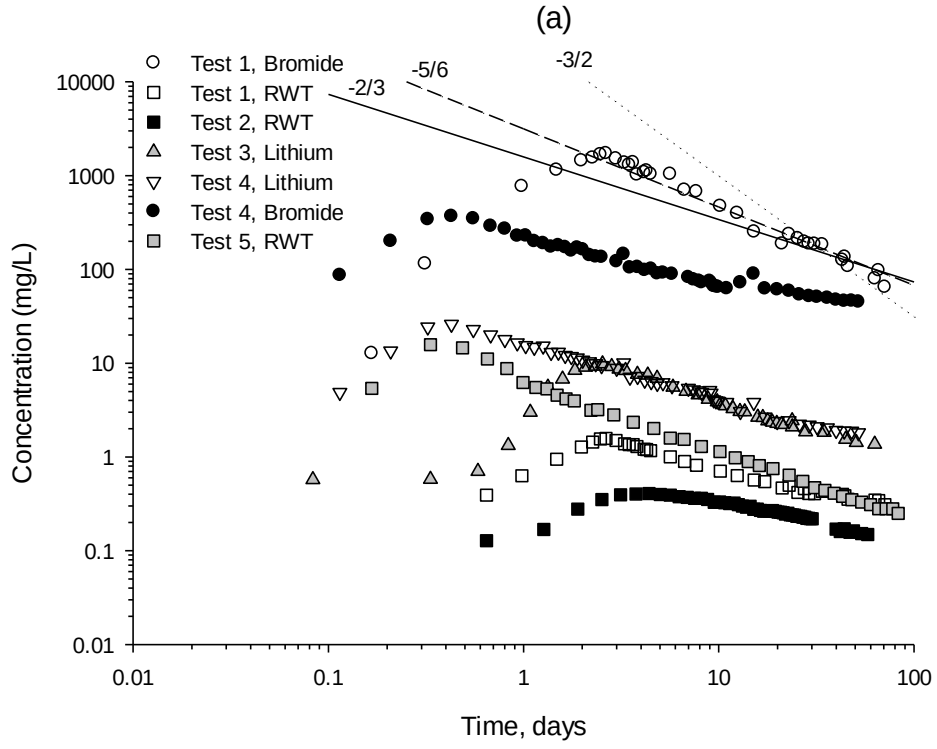

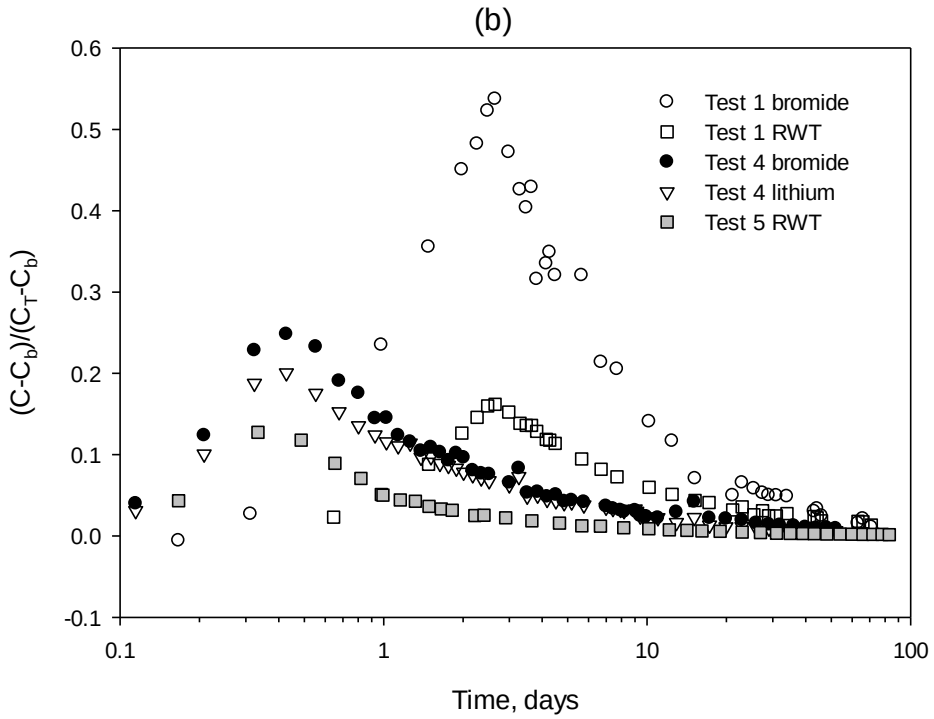

Figure 3: (a) BTCs for all tests. Straight lines are log-log gradients of -3/2 (dotted), -5/6 (dashed), -2/3 (continuous). (b) BTCs for tests 1, 4 and 5 background-corrected and normalised.

3.2. Tracer comparison

Even for conservative transport, some mass will be kept within streamtubes that do not return to the well within the duration of the experiment. Also some solute will be retarded beyond the experimental period by entering immobile zones.

Conventionally, to assess whether a tracer has passed through a medium conservatively, a mass balance is made of the proportion of the abstracted mass of tracer to that originally injected. This is more difficult for a doublet and additionally for a recirculating system since mass which has been abstracted is fed back into the system. Nonetheless, it is still possible to assess the relative performance of tracers. Given that bromide has previously been established as a conservative tracer in MSW (Woodman *et al.*, 2015), it provides a useful reference from which to compare the other tracers.

In Test 1, bromide and RWT were injected simultaneously. Comparison of the BTCs which have been background corrected and then normalised to the input tracer concentration shows different behaviour for the two tracers (Figure 3b). The difference cannot be explained by simple linear sorption (which would cause retardation, most obviously indicated by a delay in the time of the peak concentration) but instead indicates a *relative* loss of RWT compared to bromide.

In the same figure lithium and bromide in Test 4 can also be compared. There is a more subtle difference between the two curves, which becomes more obvious at the peak. In Test 4 LiBr was added as a salt, so the ratios of the concentrations above background of the tracer input is the same as the ratio of the atomic masses (11.5). The mean of the ratio of Br:Li for the measured input concentrations is 11.1, which is only 3 % different to the stoichiometric level. However, the mean of the Br:Li ratio for the BTC is 13.9. On the assumption that there is no increase in bromide concentration, this implies a net reduction in lithium concentrations of ~20%. This is a similar loss to those observed in carefully mass-balanced laboratory lithium tracer tests in waste (11 %-23 %,

Woodman *et al*., 2013; 28 %-32 %, Woodman *et al*., 2015). Since the rate at which this lithium apparently leaves solution is not understood, the BTC may potentially be distorted from what it would have been without such a loss. The mechanism for lithium removal has not been determined. It has been previously conjectured that lithium may be bound to biofilms growing on the waste mass (Woodman et al., 2013).

RWT tracer in Test 5 can be compared to the LiBr in Test 4 as the same pair of wells were used, albeit the injection was slightly (4%) shorter (Table 3). Significant depletion of RWT relative to both bromide and lithium occurs again in this instance. Depletion of RWT is thus observed consistently when compared to bromide, a nominally conservative tracer. As is the case for lithium, fitting models to the RWT data is likely to introduce uncertainty, given this unexplained non-conservative behaviour which may be due to a kinetic consumption process.

The absence of relative retardation in these comparisons suggests that depletion of the tracers is occurring without significant subsequent delayed release within the timescale of the tests. It was previously noticed (Woodman *et al*., 2014) that the loss of lithium tracer in a degrading MSW could be adequately described by a simple scaling of the BTC. The Test 1 RWT curves in Figure3b can be made to approximately overlie the Br curve if the assumed input concentration is reduced to 31 % of the measured input (regressing RWT vs Br gives R^2=0.96). Similarly, the Li curve would approximately overlie the Br curve if the assume lithium concentration is 80 % of the measured input (regressing gives R^2=0.98). RWT in Test 5 overlies most of the bromide data in Test 4 if it is assumed only 30 % of the true input was injected, although the peak is still too high.

In the absence of a convincing physically-based explanation, which may include a kinetic consumption process that can account for the depletion of lithium and RWT, these two tracers have not been fitted with a model of conservative transport. However, it is assumed that RWT and lithium can be used to estimate arrival times at the abstraction and observation wells.

3.3. First detection of tracers at abstraction well

Table 4 gives the first detection times (t_{fd}) at the abstraction well, which are notably short. By applying Equation [1] to the first arrival time of the RWT tracer in Test 1, gives a crude first estimate of kinematic porosity of 0.005-0.006. This is apparently indicative of a highly preferential flow system in which only a small sub-set of the porosity participates in advective flow. This estimate is later refined by modelling of the BTCs.

Table 4: first detection times and kinematic porosity estimates

Test	Well Separation, D (m)	Tracer used to make t_{fd} estimate	First detection time * t_{fd} (d)	Estimate for θ_K (-) using equation [1] †
1	10.0	RWT	0.19	0.005
2	19.9	RWT	0.78	0.005
3	19.9	Li	0.83	0.006
4	5.1	Br	0.09	0.006
5	5.1	RWT	0.05	0.006

* The first detection time is defined as the first time where concentration is greater than 1SD of the background concentration above the average background concentration (given in Table 3). Corrected by the time in the sample line to the measurement point, t_M (5.4 minutes).

† Assumes total porosity, θ =0.45, b =17.1 m Q =47.7 m^3/d.

Making the convenient assumption that t_{fd}~t_b for RWT in Test 1, Equation [1] can also be used to estimate t_b for all the other tests by scaling by the well separation, *D* (given in Table 4). Figure 4a shows that all of the measured times do not depart greatly from the (1:1) line of equality.

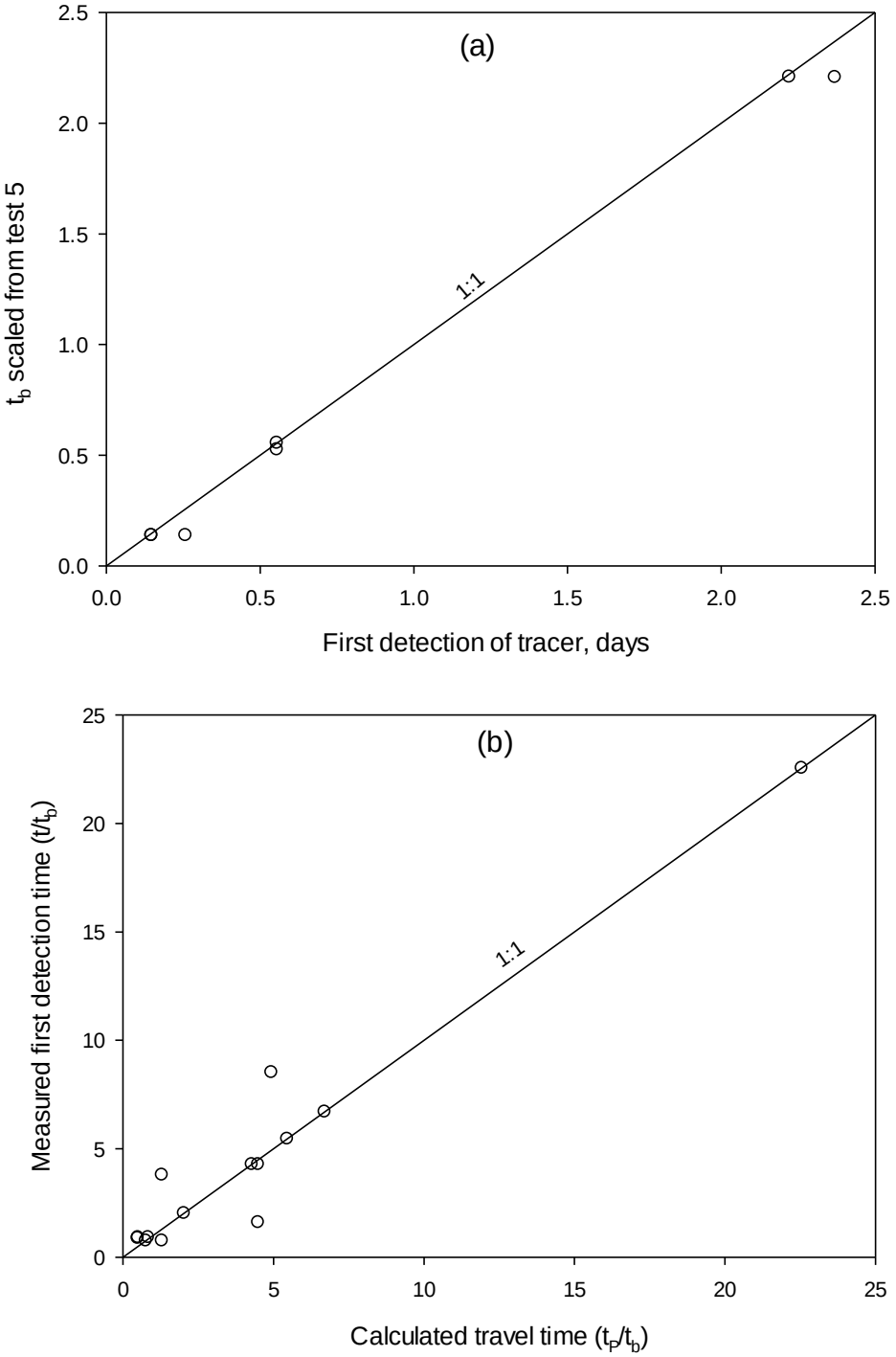

Figure 4: (a) Measured first detection time at the abstraction well (t_{fd}) versus estimates of t_b for all tests. For estimated t_b, kinematic porosity (θ_k) is calculated using Equation [1] assuming t_b is equal to the first detection time for test 1 RWT (i.e. t_{fd}~t_b), minus the advection time from the abstraction well to the monitoring point (t_M = 5.4 minutes). (b) Measured first detection time versus modelled

travel time at observation wells, normalised by t_b. Measured first detection time (t_{fd}) is the time at which concentrations are observed to rise above 1 SD above average background.

3.4. Tracer detection at observation wells

Test 4 was the only test where bromide was measured at the observation wells. Unlike RWT for which depth-profiles were taken, bromide was only measured in the observation wells at a single depth. These bromide BTCs are simulated in section 3.6.

For the tests that used it (1, 2 & 5), RWT depth profiles were taken in the observation wells. Figure 5 shows profiles of RWT during Test 1, where solute was injected at well B and removed from AW. The RWT profile in well A (midway between the two pumping wells) initially shows a uniform increase in tracer with depth along the borehole inferring that the tracer has spread throughout the saturated thickness of the waste and is travelling at uniform velocity with depth. After 24 hours there is a smooth decline in concentrations from shallow depth to the base of the well. This pattern persists for 48 hours and is maintained as the plume passes the well when concentrations at all levels begin to decline. This may possibly indicate slightly faster flow rates at shallower depths. Figure 5 also shows the profiles converted into BTCs at different depths. If different layers were transporting fluid at different rates the BTCs at slower horizons would be expected to be delayed relative to the faster horizons and this asymmetric pattern would exist from the start of the test. However, whilst the BTCs are scaled in terms of concentration, they are not delayed relative to each other. Loss of RWT at greater depth would be a mechanism that would explain such an effect, but is currently unvalidated.

The advection time, t_P, from the injection well to point P can be calculated (e.g. Muskat, 1937) and compared to the observed first detection time at an observation well. This is done in Figure 4b, normalised by the between-well advection time (t_b). Albeit with some scatter, it can be seen that there is a reasonable correspondence between measured and modelled times.

In summary, the first detection times at the abstraction well and at observation wells show that the advection of tracer within the doublet is behaving approximately according to a model of a homogeneous continuum with a relatively small kinematic porosity.

(a) Well A RWT profiles	(b) Well A BTCs
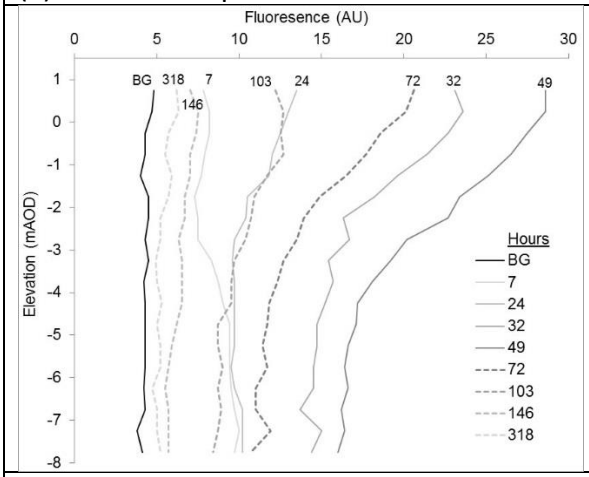	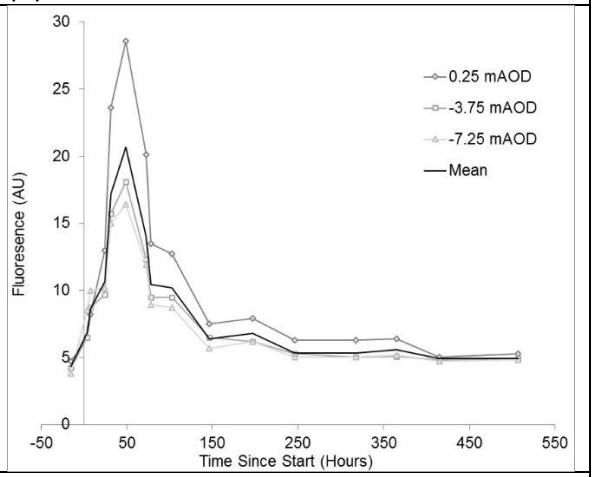
(c) Well C RWT profiles	(d) Well C BTCs

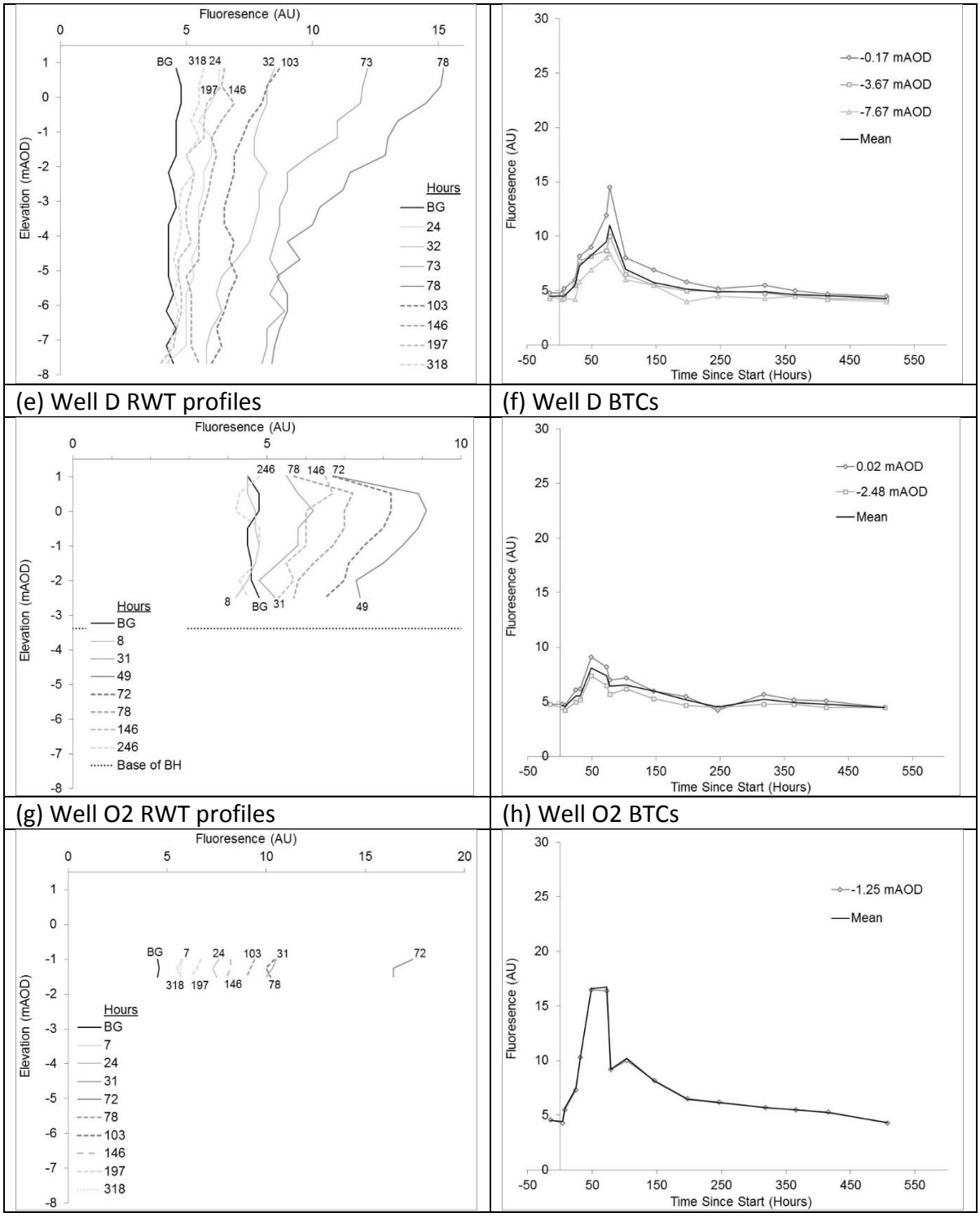

Figure 5: RWT profiles at observation wells in test 1 (doublet between AW and B) and re-plotted as BTCs at different depths and the mean concentration of all depth measurements. Fluorescence is plotted in Arbitrary Units (AU) as it was not possible to accurately convert the in situ RWT measurements to mass units owing to potential differences in temperature and turbidity. No tracer was detected in O1. Background (BG), pre-test fluorescence was measured approximately 15 hours before tracer injection. Injected Tracer had a fluorescence of ~34 AU.

3.5. Concentrations at late-times

The gradient of the BTC at late time (i.e. in the 'tail') is valuable for identifying mass-transport processes (Woodman, 2007). For example, it may distinguish aspects of diffusive transfer (Haggerty *et al*., 2000) sorption (Werth *et al*., 1997), or heterogeneous advection (Becker & Shapiro, 2000).

For one-dimensional flow, the BTC can be affected significantly by dual-porosity diffusive exchange, showing $C \sim t^{-3/2}$ in the presence of effectively infinite immobile blocks (i.e. for $t \ll t_{cb}$). This is a -3/2 log(concentration) versus log(time) gradient. Once the timescale is sufficiently long for the blocks to no longer appear infinite, exponential concentration-time gradients are observed, with the gradient depending upon the characteristic diffusion time.

The log-log gradient of concentration of a tracer moving by advection only in a doublet field is -4/3 (e.g. Barker, 2010). This power-law behaviour continues, theoretically, to infinite time. Luo *et al*. (2007) examined the effect of dual-porosity (diffusive exchange) upon the late-time gradient in a dipole. They showed that a log-log gradient of -7/6 occurs for $t_b \ll t \ll t_{cb}$. The power-law behaviour that arises due to diffusion into an effectively infinite block therefore combines with the power-law behaviour due to the geometry of the doublet, the combined exponent being $-1 - \beta(\gamma - 1)$, where $\beta = 1/2$ is due to diffusion in an effectively infinite block and $\gamma = 4/3$ is due to advective flow around a doublet (Luo *et al*., 2007).

The persistence of the power-law behaviour due to the advective flow in a doublet means that even when the condition $t \ll t_{cb}$ no longer holds, the BTC will remain as a power law and not tend to an exponential.

Luo *et al*. (2007) demonstrated that the presence of a regional flow in addition to the doublet causes a transition to an exponential slope at very long time. This latter result corresponds to the fact that the recirculation zone has a finite area. The finite site boundaries would eventually have the same effect for a sufficiently long test.

The theoretical late-time behaviour, including gradients, for a closed-loop DP doublet have been derived and are given in Table 6. In the absence of DP effects, or when $t \gg t_{cb}$ and $t \gg t_b$, a gradient of -2/3 is predicted (i.e. the recirculation serving to double the gradient from a system without recirculation). When infinite-block (i.e. where $t_b \ll t \ll t_{cb}$) effects are important, a steeper gradient of -5/6 is predicted.

Figure 3a shows late-time gradients of -2/3, -5/6 and -3/2 in comparison to the data. A gradient of -3/2 is too steep, therefore demonstrating that a 1D pathway between the wells is unlikely (such an arrangement might occur in the event of there being a highly permeable preferential route between the wells due to heterogeneities). Whether the curves conform most closely to the -2/3 or -5/6 gradients is not unambiguously revealed. Possibly the timescale of the tests was close to the limit where t_{cb} is no longer apparently infinite and the gradient was beginning to transition from -5/6 towards -2/3.

Furthermore, the late-time gradients confirm that that the regional (ambient) flow is insignificant within the timescale of this experiment, since otherwise the gradients would have tended to an exponential. There is also no systematic difference in the gradient between tracers suggesting that any reactive process that may have operated on the tracers is relatively unimportant in terms of distorting the late-time.

Table 6: New results for the asymptotic behaviour of breakthrough curves for a doublet with dual-porosity (DP) transport behaviour. These apply to times much greater than: (a) the tracer input period ($t \gg t_T$); (b) the doublet breakthrough time ($t \gg t_b$); and (c) the time for recirculation ($t \gg t_R$). The 'finite immobile region' results can also be applied to the pure advection and to the advection dispersion (AD) transport case (Equation [8]) by setting $\sigma = 0$.

Recirculation	Immobile regions	Asymptotic concentration at monitoring point	Gradient of log c vs. log t	References for the gradient
No	Finite	$C_M \sim C_T t_T \frac{m}{\lvert\Gamma(-1/3)\rvert} \sqrt[3]{\frac{(1+\sigma)t_b}{t^4}}$	-4/3	Luo *et al.*, 2007 Barker, 2010
No	Infinite or $t \ll t_{cb}$	$C_M \sim C_T t_T \frac{m}{\lvert\Gamma(-1/6)\rvert} \sqrt[6]{\frac{t_\infty}{t^7}}$	-7/6	Luo *et al.*, 2007
Yes	Finite	$C_M \sim C_T t_T \frac{1}{m\Gamma(1/3)\sqrt[3]{(1+\sigma)t_b t^2}}$	-2/3	This work
Yes	Infinite or $t \ll t_{cb}$	$C_M \sim C_T t_T \frac{1}{m\Gamma(1/6)\sqrt[6]{t_\infty t^5}}$	-5/6	This work
$t_\infty = t_b^2/t_{cf}$ $m = \lim_{z\to 0}\left\{z^{-1/3}\left[1 - \frac{1}{\pi}\int_0^\pi \exp\left(-z\tau(\psi)\right)d\psi\right]\right\} \approx 0.9104658$				

3.6. Model fitting to breakthrough curves

The bromide data (tests 1 and 4) are fitted using Equation [2] with different streamtube transfer functions, $\bar{f}_\delta$, in Equation [5]. The fits are shown in Figure 6. Three different streamtube models are compared: advection-dispersion ('AD'), dual-porosity ('DP') and these processes combined ('AD-DP').

(a)

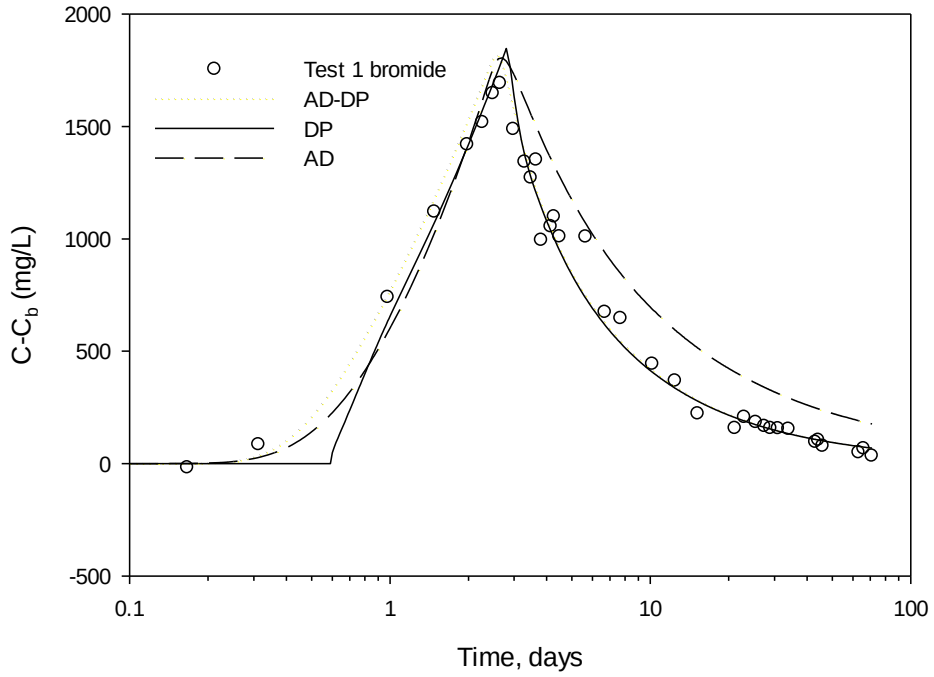
Test 1 bromide
AD-DP
DP
AD
2000
1500
1000
500
0
-500
0.1
1
10
100
C-C$_b$ (mg/L)
Time, days

(b)

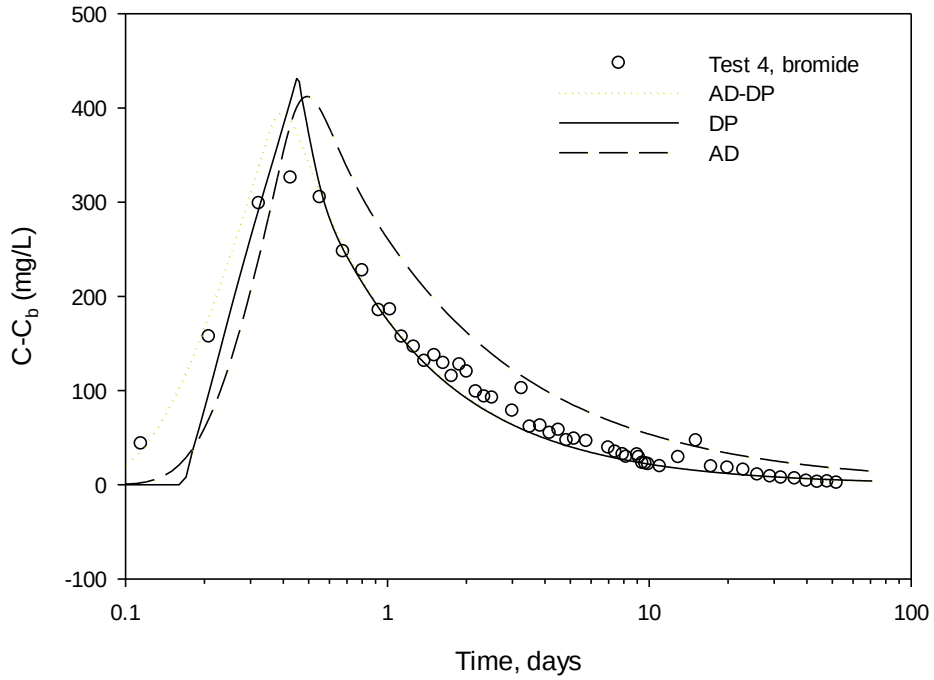
Test 4, bromide
AD-DP
DP
AD
500
400
300
200
100
0
-100
0.1
1
10
100
C-C$_b$ (mg/L)
Time, days

(c)

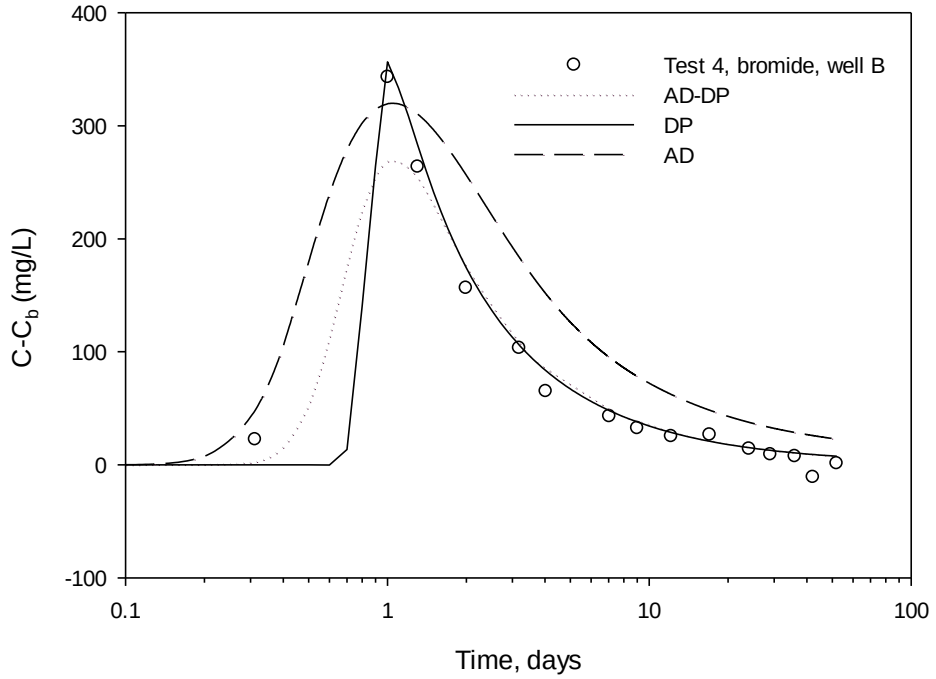

(d)

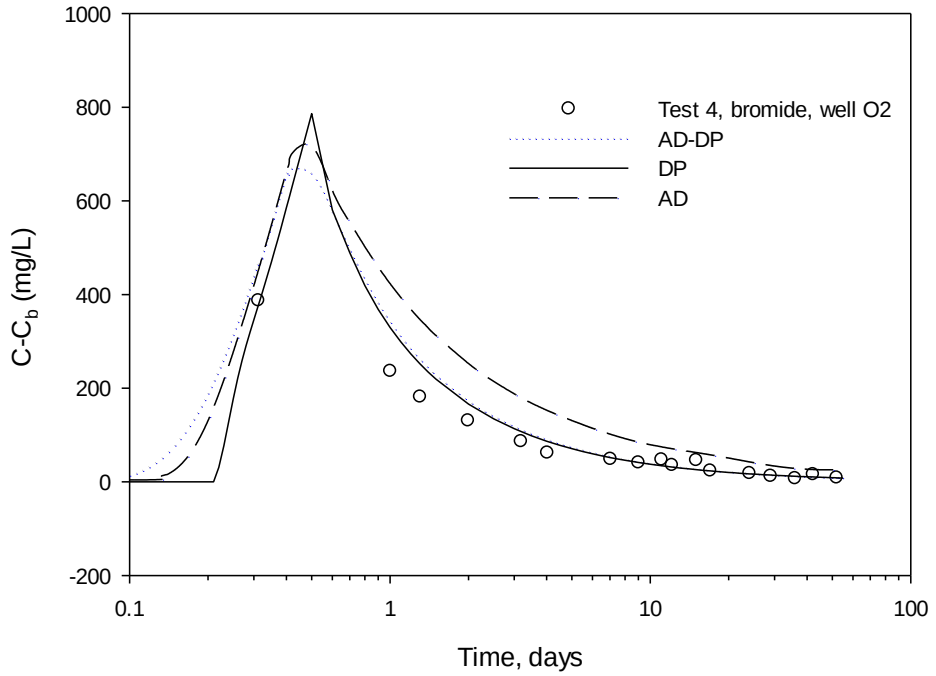

Figure 6: best fits to bromide data using the AD model (dashed line), AD-DP(infinite-block) model (dotted line) and DP (infinite-block) model (solid line). (a) Test 1 at AW, (b) Test 4 at AW, (c) Test 4 at B, (d) Test 4 at O2. Parameters for the DP model given in Table 5. For the AD-DP model, the same parameters are used, together with α/L =0.1. No adequate fits were obtained for the AD model;

the parameters giving the best sum of square fits for the AD plots given here are for α/L =0.25, 0.09, 0.54, 0.11 and t_b=1.14, 0.3, 0.19, 0.05 days for plots (a) to (d) respectively.

As is evident in Figure 6, using Equation [8] to represent advection-dispersion (AD) in each streamtube results in poor fits to the data. 'Conventional' mechanical dispersion is therefore an inadequate explanation of the movement of tracer through the system. (We also applied AD with constant dispersivity (alpha) and with alpha varying with distant but obtained similarly poor fits.)

The DP process along streamtubes is simulated using Equation [6]. Adjusting the fitting parameters t_{cb}, σ and t_b reveals that the ratio t_{cb}/σ^2 is effectively constant. This constant is the characteristic diffusion time from the mobile zone, t_{cf}. Typically, this circumstance occurs when $t \ll t_{cb}$. The timescale of the experiment is much shorter than the characteristic time for diffusion into an immobile block, which therefore appears to be effectively infinitely large. The best-fit is therefore parameterised by t_{cf} and t_b.

The abstraction well bromide data was successfully fitted by the DP model for Test 1 (R^2=0.98) and Test 4 (R^2=0.96) as detailed in Table 5. The quality of the fits to the observation well bromide data for Test 4 varied considerably between wells. The fits to well B (R^2=0.99) and well O2 (R^2=0.95) are good. Notably, the advection times estimated by all the good fits in Test 4 are close (0.09 to 0.21 days) and t_{cf} is in the range 1-3 days (Table 5). For well C there was no clear BTC measured although the model predicted a breakthrough at around 10 days (R^2=0.08). For wells D and O1 the model over-predicts the concentration peak (R^2=0.14 and R^2=0.37 respectively). Figure 6c shows the best-fit to well B and Figure 6d to well O2.

Table 5: Best fits to bromide data with dual-porosity (DP) model [*placed at end of document; landscape format*]

The RWT measurements in Test 5 provide a useful context for the bromide measurement in Test 4 because the conditions of the two tests were identical. The in-line detector facilitated measurement of the concentration profile down the length of each observation well at each measurement time. These showed an even distribution of tracer, showing no evidence for bias due to the single point measurement of bromide at the mid-depth of the wells in Test 4. The RWT BTC at well D was smooth and well-defined, yet the bromide measurement was noisy. This suggests sampling error may have affected the bromide measurements in this well, and they have not been included in the analysis. The absence of detection at C was duplicated by the RWT and again O1 was relatively attenuated compared to O2. The non-ideal behaviour at C and O1, repeated over both tracers suggests that local heterogeneities have affected the breakthrough to these wells. A single streamline samples a much smaller volume than all the combined streamlines that converge on the abstraction well and is therefore more likely to be affected by localised heterogeneities.

Working with the BTCs that were fitted adequately (in Table 5), the fitted values for t_b can be used as the basis for the estimating the mobile porosity using Equation [1]. This gives θ_m ~0.02. Previous tracer studies in waste have also indicated similar mobile porosities (Fellner, 2009 – 0.0006; Rosqvist & Destouni, 2000 – 0.02-0.13; Woodman *et al*., 2013 – 0.01; Woodman *et al*., 2015 – 0.01).

The ratio of the immobile to mobile water, σ, can be estimated by using an estimated value for the total water content θ, since $= \theta/\theta_m - 1$. By assuming θ=0.45 (Beaven et al., 2011;Beaven, 2000), σ is estimated to lie in the range 35 to 74 over these four tests. In turn, these estimates of σ together with the t_{cf} estimates can be used to estimate the block diffusion time, via the relationship $t_{cb} = \sigma^2 t_{cf}$. Using the modelled t_b as a basis for the porosity estimates, t_{cb} is estimated to be in the range 384 to 3,052 days, which is always at least seven times greater than the duration of the

experiment and explains why it could not be uniquely identified as a simple fitting parameter of the BTC.

The ability to make these later estimates is counter-intuitive given the earlier observation that the immobile blocks appear to be effectively infinite at the timescale of the tests. The additional constraint that allows this uncertainty to be removed is that the key parameters of the system (saturated depth, pumping rate, saturated water content) are already well-constrained. Analogously, solute diffusion times in the laboratory into blocks of chalk of known porosity and dimensions can be estimated from short-duration tests where only t_{cf} is measured by the tracer, but the t_{cb} can then be calculated based on the known geometry (Gooddy *et al.*, 2007).

The combined model whereby there is mechanical dispersion in a mobile zone and dual-porosity exchange with a less mobile zone ('AD-DP', Equation [10]) makes an improvement to the very early-time data, but otherwise makes insignificant difference in the fit to the peak and tail. For long-term simulations therefore the DP model is found to be adequate without the inclusion of mechanical dispersion.

The significance of mixing in the injection and abstraction wells was examined by varying the respective characteristic mixing times, t_A and t_I. Because both $t_A \ll t_b$ and $t_I \ll t_b$ the mixing in the well had very little influence on the fitting parameters and we conclude that the nature of mixing (or otherwise) in the wells has only a very minor effect.

4. Discussion

The above observations and application of models combine to produce a coherent interpretation of mass transport in MSW under a doublet flow regime.

Solute was observed to move to outlying observation wells and to abstraction wells at different separations as predicted by a simple doublet model where tracer concentration is assumed to be uniformly distributed through the saturated thickness. Although some variation was observed in vertical concentration profiles within the wells, there was no evidence of the tracer being persistently confined to narrow horizons or for bypassing in a lateral sense.

The observed advective travel times infer that the kinematic porosity (i.e. the mobile water content, θ_m) is around 0.02. This implies that the remaining water is less-mobile, and thus that diffusive exchange between the two is likely to be important.

Depth-profile data indicated that there may have been a small decrease in flow rate with depth. This would effectively serve to increase the dispersivity in the AD model.

The AD fits to the tracer data, however, were poor, and were notably worse than for those reported in tracer tests at the at the laboratory scale (Woodman *et al.*, 2015). This is likely to be because closed-loop configuration will tend to exacerbate differences between modelled residence-times, thereby worsening the fit under closed-loop conditions.

The bromide BTCs were best-fitted by a DP model which had an effectively infinite block diffusion time (t_{cb}) in relation to the duration of the test. This is consistent with the gradient of the BTC tail, which was close to the expected gradient for a closed-loop doublet-DP system with an infinite block time (-5/6). The fitting of a DP system where the block times are effectively infinite directly reveals the characteristic time for diffusion from/to the mobile zone (t_{cf}). Since the diffusive flux from a constant concentration in the mobile zone into a finite slab falls to 1 % below the rate that would occur into an infinite block in approximately time $5t_{cb}$, this suggests that the shortest duration of the experiments (around 50 days) was likely to be at least five times shorter than the time it would take

for diffusion to occur to or from the centre of a block. Model fitting therefore infers block diffusion times of 250 days or more.

Improving on this lower bound by using the fitted t_{cf} together with the mobile porosity estimate, a range of estimates for t_{cb} were established (384 to 3,052 days). The presence of such long diffusion times could be a serious limitation to accelerated clean-up schemes, very possibly being the rate limiting step for the more conservative species.

Using the free-water diffusion coefficient for bromide (2.1×10^{-9} m^2/s) as a first estimate of the real apparent diffusion coefficient, D_a, of bromide in leachate allows broad 'lumped' estimates of the block (half-width) dimension $b_b$to be calculated based on the estimated t_{cb}. Applying the definition, $t_{cb} = b_b^2/D_a$, gives a range of b_b of 0.26 m to 0.74 m. The presence of blocks of this approximate size would add a heterogeneity component to local measurements at observation wells and may account for some of the observed deviations from idealised concentrations. The tracer concentration profiles observed in those wells were not universally uniform and the BTCs at the observation wells did not all provide good fits to the data. However, there is no evidence to show that these departures were systematic. So, whilst caution should be expressed over predictions at particular points in space away from the abstraction well, volume-averaging appears to be sufficient that the overall transport to the abstraction well (and monitoring point) is amenable to continuum model-based prediction. This predictability is supported by the relatively large volume-sampling over a relatively deep saturated zone and between well-spaced boreholes. Thus, albeit they are a simplification, there is a reasonable basis to apply these models to designing and engineering clean-up systems based on multiple vertical wells at this site. A well separation of 5 m was sufficiently large to obtain reliable measurement of the system parameters. Whether such favourable conditions occur at other sites should be checked locally before assuming this may be generalised. In particular, heterogeneity due to large hidden hydraulic features is a persistent concern in landfills.

Echo tests, which were performed prior to the doublet tests, were modelled using a dual-porosity model (Barker *et al.*, 2000) giving reasonable fits to the data (Rees-White *et al.*, 2016 in prep.). Plotting these estimates of t_{cb}, together with estimates from ECHO tests performed in other UK sites against (a proxy of) volume of waste sampled by each test reveals an approximate log-log relationship (Figure 7). The doublet tests plot reasonably close to this line. Liu *et al*. (2004) showed a similar apparent relationship for tracer tests in fractured rock and suggested that the effect may have been due to a hierarchical double-porosity structure, where the larger the measurement scale the larger the spatial scale of block that may be encountered.

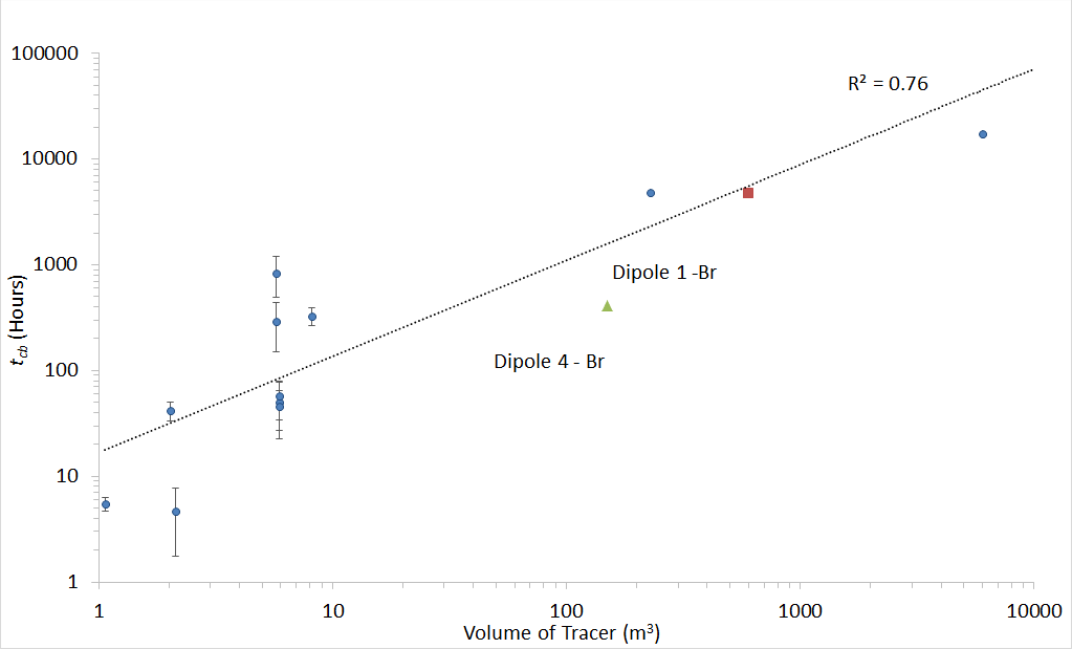

Figure 7: spatial scaling of inferred block diffusion times from tracer tests in MSW. Volume of tracer may be considered a proxy for the volume of sampled formation. Volume of tracer for the 'echo' tests (Rees-White *et al.*, 2013) estimated as volume injected (and removed). The characteristic volume of traced waste for doublet tests is estimated as the full saturated depth (17m) with total water content 0.45 and being within the circle with diameter equal to the well spacing.

Naturally, the models used here over-simplify the real conditions in the system. For example, the draw-up in the injection well and drawdown of water in the abstraction well is not explicitly dealt with in the transport equations and although this cancels out in terms of the average water level it may affect the true measured concentrations. At some stage the finite nature of the landfill will affect the outermost streamlines (at present the doublet is assumed to be on an infinite plane).

The tracers themselves were considered to be under test, in a demanding environment. RWT was depleted by ~70% and lithium was depleted by ~20% relative to bromide. RWT was therefore considered unreliable for model fitting. However, RWT was shown to be valuable for providing high-frequency measurements of breakthrough and facilitated high-resolution depth-profiles within wells.

The findings in this paper now need to be used to predict different flushing configurations. The most striking issue is the combination of a relatively small mobile porosity (~0.02) yet with long (>1 year) diffusion times. This means breakthrough of the flushing water at the abstraction well is likely to occur relatively quickly unless flow rates are sufficiently limited or wells located sufficiently far apart. Dilution of abstracted leachate with the flushing water is likely to incur additional pumping and treatment costs compared to a situation where concentrated leachate is abstracted.

Depending on the site, the optimum flushing rate may depend upon a combination of factors including the needs of the operators, the hydraulics of flow, the capacity of the treatment apparatus as well as the transport limitations outlined above (Barker & Beaven, 2010).

5. Conclusions

Well doublets were successfully used to study horizontal solute transport within a 17 m deep saturated zone in a MSW landfill. This was done since it is important to properly understand a well doublet since it is the basic unit from which a multi-well site flushing system could be built-up.

Doublets were demonstrated to be practical way to run a long duration tracer test to recover contaminant transport properties of waste. A well-doublet also forms the basic unit from which a multi-well site flushing system could be built-up, which would be one way of promoting flushing horizontally.

The results from a suite of tracer tests (borehole-dilution test, doublet tracer tests, and forced gradient tests) were self-consistent, and consistent with previous experiments in MSW. Bromide was conservative tracer, whereas RWT and lithium were shown to be relatively depleted (by ~70 % for RWT and ~30 % for lithium).

Transport of bromide tracer between an injection and an abstraction well at a range of scales (well separations of 5, 10 and 20 m) was observed to be described adequately by a simple doublet model with dual-porosity exchange between a mobile porosity (~0.02) and the remaining water content. The relatively uniform spatial tracer distribution was such that a continuum approach to transport simulation was possible, even where the well spacing was only 5 m. No 'short-circuiting' was apparent. This is likely to be due to the relatively large spatial averaging that occurs in this flow arrangement. Measurements at observation wells were broadly confirmatory of the overall conceptual model although were influenced by localised heterogeneity.

Block diffusion times were estimated between ~1 and 8 years. This is very significant for the design of horizontal field flushing systems which may be rate-limited by these diffusional effects. If the tentative scaling relationship shown in Figure 7 continues on to even greater scales, then yet longer timescales would be encountered.

The reliability of the model suggests that there is a good scope for understanding and designing horizontal flushing of contaminants by a variety of means, including injecting clean water into vertical wells and pumping leachate from additional wells.

Nomenclature

b Thickness of saturated zone [mg/L]

b_b Half-width of an immobile block [m]

B Block Geometry Function (Barker, 1985) [-]

c_X Background-corrected concentration at location X (e.g. X=M for monitoring point) [mg/L]

C_A Concentration in abstraction well [mg/L]

C_b Background concentration [mg/L]

C_I Concentration in injection well [mg/L]

C_M Concentration at the monitoring point [mg/L]

C_P Concentration at any point within the waste (e.g. at an observation well) [mg/L]

C_R Concentration returned to the injection well [mg/L]

C_T Tracer input concentration [mg/L]

D Spacing between injection and pumping well [m]

D_a Apparent diffusion coefficient [m^2/d]

M Transfer function for transport through return pipework to monitoring point [-]

P Point in the waste (defined by horizontal coordinates x, y)

q Darcy velocity [m/d]

Q Pumping (and injection) flow rate [m^3/d]

r_w Well radius [mm]

$\mathrm{R}(s)$ Transfer function for transport through return pipework to injection well [-]

s Laplace variable [d^{-1}]

s_d Slope of ln(concentration) against time in a dilution test [log(mg/L)/d]

t Time [d]

$t_a(\psi)$ Advection time for a streamtube [d]

t_A Time constant of abstraction well [d]

t_b Time for fastest advection of tracer from injection to abstraction well [d]

t_{cb} Characteristic diffusion time to/from immobile zone [d]

t_{cf} Characteristic diffusion time to/from mobile zone [d]

t_{fd} Time of first detection of tracer [d]

t_I Time constant of injection well [d]

t_M Advection time from abstraction well to monitoring point [d]

t_P Advection time from injection well to point P in waste [d]

t_R Return time from abstraction well to injection well [d]

t_T Duration of tracer input for a top-hat input [d]

$\mathrm{T}(s)$ Transfer function for transport from tracer injection point to injection well [-]

$\mathrm{W}(s)$ Transfer function for transport through waste

z Distance along a streamtube [m]

α Dispersivity [m]

α_L Dispersivity per unit distance of travel, α /z [-]

γ Specific weight [N/m^3]

θ Total volumetric water content (porosity) [-]

θ_{im} Immobile volumetric water content (porosity) [-]

θ_k Kinematic porosity [-]

θ_m Mobile volumetric water content (porosity) [-]

ψ Angle from line joining doublet wells to streamline entering abstraction well [radians]

Acknowledgements

This work was supported by EPSRC platform grant: 'Processes, mechanics & management of residual wastes' (EPSRC GR/T25194/01).

Harvey Skinner is thanked for his invaluable work building and commissioning field instrumentation, and James Rollinson for his contribution to dilution tests.

Veolia Environmental Services' ongoing support of landfill research undertaken by the University of Southampton is gratefully acknowledged.

Data statement

Relevant data supporting this study are openly available from the University of Southampton repository at http://dx.doi.org/10.5258/SOTON/400834.

References

Barker, J. A. (1985), Block-geometry functions characterizing transport in densely fissured media, *Journal of Hydrology*, *77*, 263-279.

Barker, J.A., Wright T.E.J. & Fretwell, B.A. (2000), A pulsed-velocity method of double-porosity solute transport modelling. Tracers and Modelling in hydrogeology, IAHS Publication No. 262, pp 297 – 302. Proceedings of Tra'M 2000 conference, Liege, Belgium.

Barker, J. A. (2010), Modelling doublets and double-porosity, *Quarterly Journal of Engineering Geology and Hydrogeology*, *43*, 259-268, doi:10.1144/1470-9236/08-095.

Barker, J. A., and R. P. Beaven (2010), Scientific and management concepts in landfill flushing: pilot studies using a dual-porosity model, in *Proceedings Waste 2010: Waste and Resource Management – Putting Strategy into Practice*, edited, Stratford-upon-Avon, Warwickshire, England.

Beaven, R. P. (2000), The hydrogeological and geotechnical properties of household waste in relation to sustainable landfilling, PhD thesis, University of London, London.

Beaven, R. P., J. A. Barker, and A. Hudson (2003), Description of a tracer test through waste and application of a double porosity model, paper presented at Sardinia 2003: Proceedings of the Ninth International Waste Management and Landfill Symposium, Margherita di Pula, Cagliari, Sardinia, Italy.

Beaven, R. P., K. Knox, and B. Croft (2001), Operation of a leachate recirculation trial in a landfill test cell, paper presented at Sardinia 2001, International Waste Management and Landfill Symposium, S. Margherita di Pula, Cagliari, Sardinia, Italy.

Beaven, R. P., K. Knox, J. R. Gronow, O. Hjelmar, D. Greedy, and H. Scharff (2014), A new economic instrument for financing accelerated landfill aftercare., *Waste Management*, *34*(7), 1191-1198.

Beaven, R.P., Powrie, W. and Zardava, K. Hydraulic properties of MSW. In Geotechnical characterization, Field Measurements and Laboratory Testing of Municipal Solid Waste - Zekkos, Dimitrios (ed.) 2011 Published by: Virginia, US. Series: ASCE Geotechnical Special Publication, 209 pp. 1-43

Beaven, R. P., J. K. White, and S. A. Q. Burton (2004), The effect of moisture content in controlling landfill gas production and its application to a model for landfill refuse decomposition, in *Waste 2004*, edited, pp. 333-342., Stratford-upon-Avon.

Becker, M. W., and A. M. Shapiro (2000), Tracer transport in fractured crystalline rock: evidence of nondiffusive breakthrough tailing, *Water Resources Research*, *36*(7), 1677-1686.

Bendz, D., V. P. Singh, H. Rosqvist, and L. Bengtsson (1998), Kinematic wave model for water movement in municipal solid waste, *Water Resources Research*, *34*(11), 2963-2970.

Bhada-Tata, Perinaz, Hoornweg, and D. A.. (2012), What a waste?: a global review of solid waste management *Rep.*, World Bank Group. , Washington, DC.

Blakey, N. C., K. Blackmore, and L. Clarke (1998), Application of tracer studies for monitoring leachate recirculation in landfills*Rep. CWM 171/98*, Environment Agency, Report CWM 171/98.

Burrows, M. R. (1998), Landfill hydrogeology and the hydraulic properties of in-situ landfilled material. PhD Thesis, Royal Holloway, University of London.

Burrows, M. R., J. B. Joseph, and M. J. D. (1997), The hydraulic properties of in-situ landfilled waste., in *Sardinia 97. S. Margherita di Pula, Cagliari, Italy.*, edited.

Christensen, T. H., S. Manfredi, and P. Kjeldsen (2011), Landfilling: environmental issues, in *Solid waste technology & management*, edited by T. H. Christensen, Blackwell Publishing Ptd, Chichester, UK.

Cossu, R., G. Fongia, A. Muntoni, A. Mobile, and R. Raga (1997), Use of pumping tests for the assessment of leachate flow regime, waste hydraulic parameters and well efficiency, in *Sardinia 97.* , edited, S. Margherita di Pula, Cagliari, Italy.

Drury, D., D. Hall, and J. Dowle (2003), The development of Landsim 2.5 *Rep. NGWCLC GW/03/09*, Environment Agency

Fellner, J. (2009), Comparing field investigations with laboratory models to predict landfill leachate emissions, *Waste Management*, *29*, 1844–1185.

Fellner, J., and P. Brunner, H. (2010), Modeling of leachate generation from MSW landfills by a 2-dimensional 2-domain approach, *Waste Management*, *30*(11), 2084-2095 doi:10.1016/j.wasman.2010.03.020.

Flury, M., and H. Flühler (1995), Tracer characteristics of Brilliant Blue FCF, *Soil Sci. Soc. Am. J.*, *59*, 22-27.

Giardi, M. (1997), Hydraulic behaviour of waste: observations from pumping tests., in *Sardinia 97, Sixth International Landfill Symposium,*, edited, pp. 63-72, S Margarita de Pula, Cagliari, Sardinia, Italy.

Gooddy, D.C., Kinniburgh, D.G. and Barker, J.A. (2007), A rapid method for determining apparent diffusion coefficients in Chalk and other consolidated porous media. *Journal of Hydrology*, 343:97-103.

Haggerty, R., S. A. McKenna, and L. C. Meigs (2000), On the late-time behavior of tracer test breakthrough curves, *Water Resources Research*, *36*(12), 3467-3479.

Hall, D. H., J. Gronow, R. Smith, and N. Blakey (2004), Achieving equilibrium status and sustainable landfill - the holy grail?, paper presented at Waste 2004. Integrated Waste Management and Pollution Control: Policy and Practice, Research and Solutions., Stratford-upon-Avon, UK.

Harris, M. R. R. (1979), A study on the behaviour of refuse as a landfill material, PhD thesis, Portsmouth Polytechnic.

Hoopes, J. A., and D. R. F. Harleman (1965), Waste water recharge and dispersion in porous media. *Rep. Tech. Rep. No 75*, Hydrodynamic lab, MIT, Cambridge, Massachusetts.

Jury, W. A., and K. Roth (1990), *Transfer Functions and Solute Transport Through Soil: Theory and Applications.*, Birkhaeuser Publ. Basel. 235 p.

Kattenberg, W. J., H. A. van der Sloot, and T. J. Heimovaara (2013), New Dutch legislation to allow research of natural biodegradation at landfills, in *Proceedings Sardinia 2013, Fourteenth International Waste Management and Landfill Symposium*, edited, S. Margherita di Pula, Cagliari, Sardinia, Italy.

Lee H, Lee Y, Kim J & Kim C (2014) Field Application of Modified In Situ Soil Flushing in Combination with Air Sparging at a Military Site Polluted by Diesel and Gasoline in Korea, International Journal of Environmental Research and Public Health, 11(9): 8806–8824.

Liu, H. H., G. S. Bodvarsson, and G. Zhang (2004), Scale dependency of the effective matrix diffusion coefficient, *Vadose Zone Journal*, *3*, 312-315.

Luo, J., and K. Kitanidis (2004), Fluid residence times within a recirculation zone created by an extraction–injection well pair, *Journal of Hydrology*, *296*, 149-162.

Marius, M., A. Stringfellow, D. Smallman, and T. Atkinson (2010), Fluorescent tracers - a tool for landfill investigation and management, in *Waste 2010, Waste & Resource Management: putting strategy into practice.* , edited, pp. 69-67-, Stratford-on-Avon.

Muskat, M. (1937), *The flow of homogeneous fluids through porous media*, McGraw-Hill, New York.

Öman, C., and H. Rosqvist (1999), Transport fate of organic compounds with water through landfills, *Water Research*, *33*(10), 2247-2254.

Powrie, W., and R. P. Beaven (1999), Hydraulic properties of household waste and implications for landfills, *Proc. Instn Civ. Engrs Geotech. Engng*, *137*, 235-247.

Press, W. H., S. A. Teukolsky, W. T. Vetterling, and B. P. Flannery (1992), *Numerical recipies in C*, Cambridge University Press, Cambridge.

Rees-White, T. (2007), Improving yields from vertical landfill wells through better design, installation and maintenance, PhD thesis, University of Southampton, Southampton.

Rees-White, T., Woodman, N.D. and Beaven, R.P. (2013), Evaluating echo tests as a landfill contaminant transport characterisation tool. In: J. MacDougall (Editor), 5th International Workshop Hydro-Physico-Mechanics of Landfill, , Napier University, Edinburgh.

Rollinson, J., T. Rees-White, J. A. Barker, and R. P. Beaven (2010), A single borehole dilution technique to measure the hydrogeological properties of saturated landfilled waste, in *Waste 2010: Waste and Resource Management – Putting Strategy into Practice*, edited, Stratford-upon-Avon, Warwickshire, UK.

Rosqvist, H., and G. Destouni (2000), Solute transport through preferential pathways in municipal solid waste, *Journal of Contaminant Hydrology*, *46*, 39-60.

Rosqvist, H., and D. Bendz (1999), An experimental evaluation of the solute transport volume in biodegraded municipal solid waste, *Hydrology and Earth System Science*, *3*(3), 429-438.

Rowe, K. (2005), Long-term performance of contaminant barrier systems, *Geotechnique*, *55*(9), 631-678.

Scharff, H., A. van Zomeren, and H. A. van der Sloot (2011), Landfill sustainability and aftercare completion criteria. , *Waste Management & Research*, *29*(1), 30-40.

Smart, P. L. (1985), Applications of Fluorescent Dye Tracers in the Planning and Hydrological Appraisal of Sanitary Landfills, *Quarterly Journal of Engineering Geology and Hydrogeology*, *18*, 275-286.

Stegemann, J. A., J. Lin, and R. P. Beaven (2006), Preliminary investigation of the sorption of common landfill tracers to MSW, paper presented at Waste 2006, Stratford-Upon-Avon.

Taylor, G. I. (1954) The Dispersion of Matter in Turbulent Flow through a Pipe. *Proceedings of the Royal Society of London. Series A, Mathematical and Physical Sciences*, Vol. 223, No. 1155, pp. 446-468.

Turner, D. A., R. P. Beaven, and N. D. Woodman (2016), Evaluating landfill aftercare strategies: a life-cycle assessment approach, *Waste Management*, *Submitted*

US EPA (2011) Background information document for life-cycle inventory landfill process model. Durham, NC, USA: United States Environmental Protection Agency.

United Nations, (1987) Our Common Future - Brundtland Report. Oxford University Press, p. 204.

Ward, R. S., J. A. Barker, A. T. Williams, L. J. Brewerton, and I. N. Gale (1998), Groundwater Tracer Tests: a review and guidelines for their use in British Aquifers, *Rep. WD/98/19 Hydrogeology Series*, BGS.

Werth, C. J., J. A. Cunningham, P. V. Roberts, and M. Reinhard (1997), Effects of grain-scale mass transfer on the transport of volatile organics through sediments, *Water Resources Research*, *33*(12), 2727-2740.

Woodman, N. D. (2007), Modelling of transport in heterogeneous porous media with application to solute transport in landfills, PhD thesis, University College London, London.

Woodman, N. D., T. Rees-White, A. Stringfellow, R. P. Beaven, and A. P. Hudson (2015), Multiple-tracer tests for contaminant transport process identification in saturated municipal solid waste, *Waste Management*, *38*, 250–262, doi:http://dx.doi.org/10.1016/j.wasman.2014.12.012.

Woodman, N. D., T. Rees-White, A. Stringfellow, R. P. Beaven, and A. P. Hudson (2014), Quantifying the effect of compression on solute transport through degrading municipal solid waste, *Waste Management*, *34*(11), 2196-2208.

Woodman, N. D., A. A. Siddiqui, W. Powrie, A. Stringfellow, R. P. Beaven, and D. J. Richards (2013), Quantifying the effect of settlement and gas on solute flow and transport through treated municipal solid waste, *Journal of Contaminant Hydrology*, *153*, 106-121 doi:10.1016/j.jconhyd.2013.04.007

Table 3: tracer injection details.

Test	Tracer	Tracer purity, supplier.	Average background in abstraction well (SD in brackets) (mg/L)	Average background in observation wells. (SD in brackets) (mg/L)	Mass added (g)	Target conc. above background (mg/L)	Injected conc. * (mg/L)	Well spacing (m)	Duration of tracer injection (hours)
1	RWT	20 % solution, Tolbest Ltd.	0.194 (0.025)	-	899.9	8.3	9.1	10.0	54.25
1	Br (as KBr)	99.92 %, ABSCO Ltd.	30.47 (1.71)	-	218,027	2022.0	a. 3181.7† b. 2098.0†	10.0	54.25
2	RWT	20 % solution, Tolbest Ltd.	0.126 (0.028)	-	1000	17.7	17.7	19.9	28.33
3	Li (as LiCl)	99 %, ABSCO Ltd.	0.629 (0.05)	0.666 (0.05)	5389	158.0	174.8	19.9	17.08
4	Li (as LiBr)	99 %, ABSCO Ltd.	0.955 (0.099)	1.046 (0.021)	1563	113.0	125.5	5.1	6.93
4	Br (as Li Br)	99 %, ABSCO Ltd.	31.67 (2.51)	32.73 (3.07)	17990	1301.0	1393.5	5.1	6.93
5	RWT	20 % solution, Tolbest Ltd.	0.037 (0.005)	0.04 (0.01)	919	69.0	128.0	5.1	6.67

* mean of measurements, for $t < t_{fd}$.

† first measurement (a) was repeated giving concentration (b). In the repeat measurement, samples were filtered and the effect of an erroneous indium internal standard was removed. The full BTC used in this paper is from the first measurement, factored by the ratio of these measurements.

Table 5: Best fits to bromide data with dual-porosity (DP) model (standard error of fit in brackets). M is the monitoring point on the return line between the abstraction and injection wells. Separation, D, for DPT1 is 10 m and for DPT4 is 5 m. Q=47.9 m^3/d, θ=0.45. Mixing in the injection and abstraction wells is neglected ($t_I = t_A = 0$), the recirculation time (t_R) is 0.01 days. Effectively infinite immobile blocks are assumed. Fits to well C, D and O1 were too poor to give parameters (R^2=0.08, 0.14 and 0.37 respectively).

Test	Observation point	Background conc. C_b (fixed)	Injected tracer conc. C_T (fixed)	t_b (d)	t_{cf} (d)	σ estimated (-)	θ_m estimated (-)	t_{cb} estimated (d)	R^2 (-)
1	M	30.47	3151.2	0.58 (0.03)	4.2 (0.83)	34.6	0.016	3052	0.98
4	M	32.73	1360.8	0.17 (0.01)	0.9 (0.19)	73.8	0.021	384	0.96
4	B	32.73	1360.8	0.15	2.0	49.9	0.015	1761	0.99
4	O2	32.73	1360.8	0.09	3.1	40.0	0.011	914	0.95